Uncertainty Quantification of the Crosstalk in Multiconductor Transmission Lines via Degree Adaptive Stochastic Response Surface Method

Quanyi Yu [1], Wei Liu [2], Kaiyu Yang [2], Xilai Ma [3], and Tianhao Wang [1*]

[1] College of Instrument Science and Electrical Engineering
Jilin University, Changchun, 130026, China
wangtianhao@jlu.edu.cn

[2] College of Automotive Engineering
Jilin University, Changchun, 130022, China

[3] Commercial Vehicle Development Institute Electric Department
FAW JIEFANG, Changchun, 130011, China

Abstract ― The degree adaptive stochastic response surface method is applied to analyze statistically the crosstalk in multiconductor transmission lines (MTLs). The coefficient of polynomial chaos expansion (PCE) is obtained based on the least angle regression. The truncation degree of PCE is iterated using the degree adaptive truncation algorithm, and the optimal proxy model of the crosstalk of the original MTLs that satisfies the actual error requirements is calculated. The statistical properties of crosstalk in MTLs (such as mean, standard deviation, skewness, kurtosis, and probability density distribution) are obtained. The failure probability of the electromagnetic compatibility in the MTLs system is considered. The global sensitivity indices of crosstalk-related factors are analyzed. Finally, the proposed method is proved to be effective compared with the conventional Monte Carlo method. The uncertainty quantification of crosstalk in MTLs can be calculated efficiently and accurately.

Index Terms ― Crosstalk, degree adaptive, multi-conductor transmission lines (MTLs), statistical property, stochastic response surface method.

I. INTRODUCTION

Crosstalk in multiconductor transmission lines (MTLs) is one of the main electromagnetic compatibility (EMC) problems in various electronic and electrical systems and devices. When predicting the crosstalk of systems or devices under actual conditions, the geometric parameters of MTLs and electrical parameters of load components related to crosstalk will be uncertain because of objective factors. This uncertainty increases considerably the difficulty of crosstalk prediction and causes the performance of crosstalk cancelling algorithms with certain parameters [1]–[2] to decrease. Therefore, to ensure EMC performance of a system or equipment, studying the statistical property of crosstalk in MTLs is very important. This problem has been explored extensively and some results have been obtained. The conventional Monte Carlo (MC) method can be used to analyze crosstalk models statistically with random input variables [3]–[5]. Although results obtained under a large number of samples are more accurate, MC is difficult to apply when using the crosstalk of large-scale systems or equipment because of its large consumption of computing resources and inefficiency. Therefore, classical reliability methods, such as first order reliability method, second order reliability method, stratified sampling, and importance sampling [6]–[7], and numerical integration methods, such as full factor numerical integration and coefficient grid numerical integration [8], have been proposed to analyze the uncertainty of crosstalk. Several other stochastic methods [9]–[11], have been applied for this analysis. The computational efficiency has been improved considerably compared with the MC method, but the statistical moments, EMC failure probability, and sensitivity analysis of crosstalk statistics have not been studied fully.

The polynomial chaos expansion (PCE) has been used widely in analyzing the uncertainty of the crosstalk in MTLs. The PCE has a solid mathematical foundation and can obtain a "cheap" proxy model of the original output response [12]. With this proxy model, the statistical moments of the crosstalk in MTLs, the failure probability of EMC, and the calculation of sensitivity analysis can be determined [13–15]. However, existing related studies only predict and verify the case where the model expansion degree is fixed within the full

Submitted On: July 5, 2020
Accepted On: January 18, 2021

https://doi.org/10.47037/2020.ACES.J.360209

frequency range of the simulation. The relationships among the model complexity, deployment degree, and calculation accuracy have not been discussed in depth. This paper will report an in-depth study on this problem.

Dr. Isukapalli of the New Jersey State University first proposed the stochastic response surface method (SRSM) [16], which belongs to the non-intrusive polynomial chaos method. The SRSM is highly similar to the deterministic response surface method. The difference between these methods is that the response surface of SRSM is constructed in the stochastic probability space. PCE coefficients are obtained based on linear regression and can be used to solve engineering uncertainty. Blatman *et al*. [17] proposed an adaptive PCE method based on linear regression to minimize the number of evaluations of the complex models. This method belongs to SRSM, but the degree of the model is obtained by the degree adaptive algorithm, and the least angle regression (LAR) algorithm is used when the model depends on numerous parameters to enable a better solution for the high-degree uncertainty [18]. This method has been applied successfully in many fields [19]–[20]. In this paper, the degree adaptive stochastic response surface (DA-SRSM) is proposed and used for the first time to solve the high-degree problem caused by the high complexity of the model of the uncertainty of crosstalk in MTLs. The proposed method provides an effective scheme for the uncertainty analysis of complex stochastic crosstalk model.

In this work, DA-SRSM is applied to analyze the uncertainty of crosstalk in MTLs. The statistical moment information can be directly calculated from the PCE coefficients, whereas the EMC failure probability of the system is calculated by using the PCE model obtained. Combined with the global sensitivity analysis via the Sobol method, the degree of influence of each random input variable on the crosstalk variation is obtained. In Part II, the analysis method of engineering uncertainty based on the DA-SRSM method is introduced and the three-conductor transmission lines model established in Part III is explored. In Part IV, the simulation results of the proposed method are compared with the MC method to verify the accuracy and validity of the proposed method. In Part V, relevant conclusions of this paper are provided.

II. DEGREE ADAPTIVE STOCHASTIC RESPONSE SURFACE METHOD

A. SRSM based on LAR

SRSM, as a non-intrusive approach, considers the complex response function as a black box when analyzing the engineering uncertainty problems and focuses only on the mapping relationship between the input and output. This method solves the PCE coefficient based on linear regression. By approximating the output of the stochastic system with the PCE model, the SRSM provides an efficient method for uncertainty propagation [21]. The LAR method is selected for linear regression. The flow chart of SRSM is shown in Fig. 1.

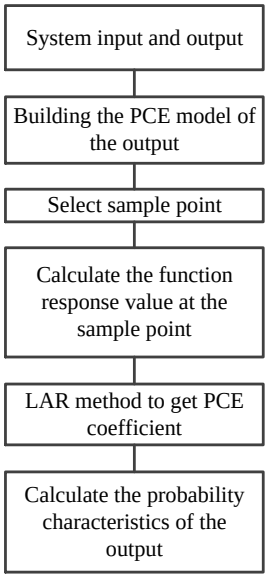

Fig. 1. SRSM flowchart.

First, a stochastic response surface is constructed. The output $Y(\theta)$ of the original model is represented as a general polynomial chaos model [22]:

$$\begin{aligned} Y(\theta) &= b_0 I_0 + \sum_{i_1=1}^{\infty} b_{i_1} I_1\left(\xi_{i_1}(\theta)\right) \\ &+ \sum_{i_1=1}^{\infty}\sum_{i_2=1}^{i_1} b_{i_1 i_2} I_2\left(\xi_{i_1}(\theta),\xi_{i_2}(\theta)\right) \\ &+ \sum_{i_1=1}^{\infty}\sum_{i_2=1}^{i_1}\sum_{i_3=1}^{i_2} b_{i_1 i_2 i_3} I_3\left(\xi_{i_1}(\theta),\xi_{i_2}(\theta),\xi_{i_3}(\theta)\right)+\cdots \\ &= \sum_{i=0}^{\infty} \hat{b}_i \Phi_i(\xi). \end{aligned} \tag{1}$$

In (1), $I_n\left(\xi_{i_1},\cdots,\xi_{i_n}\right)$ represents a mixed orthogonal polynomial of n degree. This equation is a function of multi-dimensional standard random variables $\left[\xi_{i_1},\cdots,\xi_{i_n}\right]$. $\hat{b}_i$ and Φ_i represents the PCE coefficients and orthogonal polynomials to be solved, which correspond to $b_{i_1 i_2 \ldots i_p}$ and $I_n\left(\xi_{i_1},\cdots,\xi_{i_n}\right)$ in (1). Combined with the actual problem for the calculation accuracy requirements, the PCE model in (1) is usually truncated to a certain degree p. The corresponding p-degree PCE approximation model is expressed as follows:

$$Y = \sum_{i=0}^{P} \hat{b}_i \Phi_i(\xi). \tag{2}$$

The number Q of the PCE coefficients $\hat{b}_i$ of the p-th degree truncation increases with the degree p and the dimension d of the random variable ξ. The Q value is as follows:

$$Q = \frac{(d+p)!}{d!\,p!}. \tag{3}$$

In (2), $\Phi_i(\xi)$ is the product of the one-dimensional orthogonal polynomial basis function corresponding to each dimension of the random variable $\xi_1,\ldots,\xi_d$, which satisfies the orthogonal relationship as follows:

$$\begin{aligned} \left\langle \Phi_i(\xi)\Phi_j(\xi) \right\rangle &= \int \Phi_i(\xi)\Phi_j(\xi) W(\xi) \mathrm{d}\xi \\ &= \left\langle \Phi_i(\xi)^2 \right\rangle \delta_{ij}, \end{aligned} \tag{4}$$

where δ_{ij} is the Kronecker function, $W(\xi)$ is the weight function, and the Askey scheme [23]–[24] provides the orthogonal polynomial basis functions corresponding to the random variables of different distribution types.

After the SRSM model is constructed, the sample points are selected by Latin Hypercube Sampling, which makes the sample exhibit simultaneously good spatial and projection uniformity [25]. Refer to [26], satisfactory results can be obtained by selecting sample size of twice the PCE coefficient, and the PCE coefficient $\hat{b}_i$ is estimated by the LAR method, which was proposed by Efron *et al*. [27] in 2004. The algorithm path is shown in Fig. 2.

Step 1: The initial value of all PCE coefficients $\hat{b}_i$ is set to 0. The correlation r between the regression variable $\Phi_i(\mathrm{x})$ and the current residual e_i is calculated. The input variable X_i with the highest correlation is obtained:

$$r = \frac{Cov(\Phi_i(\mathrm{x}), e_i)}{\sqrt{Var[\Phi_i(\mathrm{x})] Var[e_i]}}. \tag{5}$$

Step 2: Perform a least squares approximation on Y along the X_i direction until the next variable x_j appears, and the residuals e of $\hat{b}_{i1}\mathrm{x}_i$ and Y have the same correlation with x_i and x_j as follows:

$$\mathrm{r}_{\mathrm{x}_i \mathrm{e}} = \mathrm{r}_{\mathrm{x}_j \mathrm{e}}, \tag{6}$$

then, the third variable along the angle bisector X_i and X_j is found.

Step 3: By analogy, until the current residual is less than a given threshold, the iteration is terminated, and the final PCE coefficient $\hat{b}_j$ is obtained.

After $\hat{b}_j$ is obtained, the PCE model of the original output response is used to analyze the subsequent uncertainties. Compared with the ordinary least squares, the PCE coefficients are obtained by the LAR algorithm when calculating high-degree problems as follows:

$$\dim_{\mathrm{b}_j}^{\wedge} << \dim_{\mathrm{b}_i}^{\wedge}. \tag{7}$$

The automatic screening of regression variables is realized and the sparse PCE model is obtained, which is more efficient in solving high-degree problems.

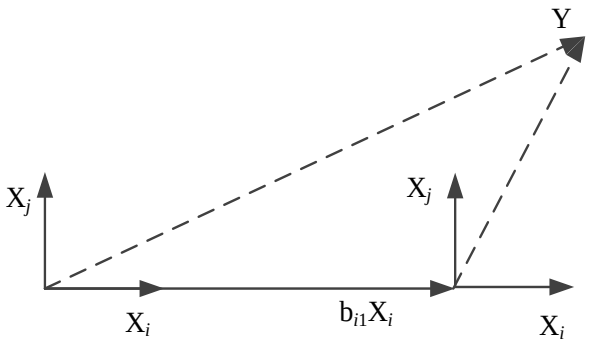

Fig. 2. LAR algorithm path.

After the PCE coefficient $\hat{b}_j$ is obtained, the first four statistical moments of the output response can be calculated. The expressions of mean μ, standard deviation σ, skewness δ, and kurtosis κ are calculated as follows:

$$\begin{cases} \mu = b_0 \\ \sigma = \sqrt{\sum_{i=1}^{p-1} \left[\mathrm{b}_i^2 \left\langle \Phi_i^2 \right\rangle \right]} \\ \delta = \dfrac{1}{\sigma^3} \sum_{i=1}^{p-1} \left[\mathrm{b}_i^3 \left\langle \Phi_i^3 \right\rangle \right] \\ \kappa = \dfrac{1}{\sigma^4} \sum_{i=1}^{p-1} \left[\mathrm{b}_i^4 \left\langle \Phi_i^4 \right\rangle \right] \end{cases}. \tag{8}$$

B. Degree adaptive truncation algorithm

The accuracy of the model determines directly the accuracy of the uncertainty analysis of the output response. In most cases, the higher the degree, the better the precision of the PCE model. The lower-degree model sometimes cannot fit the original output response well but a too high degree will lead to a waste of computing resources. Hence, to reduce the computational complexity and improve computational efficiency whereas satisfying the computational accuracy, the degree adaptive truncation algorithm [28]–[29] is used to construct the PCE model as follows:

Step 1: An initial truncation degree p_0 is set such that $p=p_0$;

Step 2: The coefficient of the p-degree PCE model and the leave-one-out (LOO) cross-validation error term e_{LOO} are calculated as follows:

$$e_{LOO} = \sum_{i=1}^{p-1} \left(\frac{Y_i - Y_i^{PC}}{1-h_i}\right)^2 / \sum_{i=1}^{p-1} (Y_i - \mu)^2, \quad (9)$$

where Y_i^{PC} is the ith PCE metamodel of the original output affecting Y_i, and h_i is the ith component of the vector h as follows:

$$A = \Phi_i(x), \quad (10)$$

$$h = \mathrm{diag}(A(A^T A)^{-1} A^T). \quad (11)$$

Step 3: e_{LOO} is compared with the threshold error e_T. If $e_{LOO} \le e_T$ or the number of defined iterations $N_{\max}$ is reached, the iteration is stopped. Otherwise, $p=p+1$ and step 2 is repeated.

Over-fitting can occur easily when the complexity of the PCE model is too high and the sample size is too small. LOO only leaves one sample as the verification set at a time, and the rest as the training set. The full use of sample data and numerous synthesis of error results can avoid over-fitting as much as possible. However, this training is time-consuming. In order to minimize the amount of calculation whereas ensuring the calculation accuracy and high computational efficiency, the earliest stopping strategy is adopted. The maximum number of iterations $N_{\max}$ is set. Whether e_{LOO} satisfies the given error criterion e_S is verified when at least two iterations e_{LOO} do not decrease or the number of iterations reaches $N_{\max}$. If this criterion is satisfied, p is accepted. Otherwise, $p=p+1$ and step 2 is repeated.

Thus, the optimal selection of the degree of the full-range PCE model under the required accuracy can be quickly realized. The complex output response can be quickly and accurately fitted.

C. Failure probability calculation of EMC performance via DA-SRSM

Usually, there are certain safety thresholds y_T for electronic and electrical systems that have EMC problems. When the input of the system is random, the output response has a small probability of exceeding y_T. When the failure probability exceeds the minimum standard in practical application, the designed electronic and electrical systems should be rectified. DA-SRSM can easily calculate the failure probability. To describe an uncertain system, a limit state function is defined as follows:

$$g(X) = y_T - Y(X), \quad (12)$$

where $Y(X)$ represents the output response of the system and y_T represents the security threshold of the system, which is generally given by numerous experimental data or empirical values. Figure 3 shows the limit state of a two-dimensional problem, and the failure probability is as follows:

$$P_f = P(g(X) < 0). \quad (13)$$

$g(X)$ is used directly as the original output response of the PCE model, and the corresponding PCE model is calculated by the DA-SRSM algorithm. The failure probability P_f of the system EMC performance is obtained by (12) combined with the PCE model.

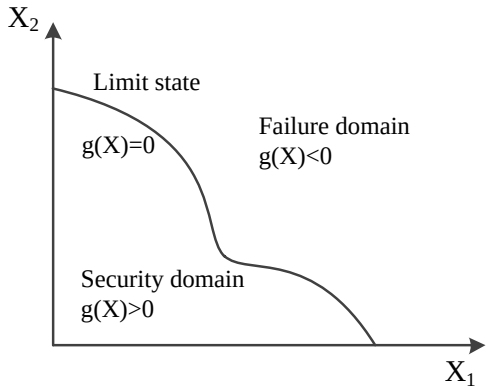

Fig. 3. Limit state concept.

D. Sensitivity analysis of Sobol via PCE

Another advantage of the proposed method is the feasibility of its combination with the Sobol method for global sensitivity analysis. The DA-SRSM is also more efficient than the conventional MC method for global sensitivity analysis. Sensitivity indices measure the influence of input variables on output response, including the first-order sensitivity and total sensitivity indices. Relevant parameters can be designed based on the sensitivity data to improve the EMC performance of the system.

Equation (2) is expanded into the Sobol decomposition form as follows:

$$\begin{aligned} Y(\xi) = b_0 &+ \sum_{i=1}^{n} \sum_{\alpha \in I_i} b_\alpha \Phi_\alpha(\xi_\alpha) + \\ &\sum_{1 \le i_1 < i_2 \le n} \sum_{\alpha \in I_{i_1,i_2}} b_\alpha \Phi_\alpha(\xi_{i_1}, \xi_{i_2}) + \cdots \\ &+ \sum_{1 \le i_1 < \cdots < n} \sum_{\alpha \in I_{i_1,\cdots,i_s}} b_\alpha \Phi_\alpha(\xi_{i_1}, \cdots, \xi_{i_s}) + \cdots \\ &+ \sum_{\alpha \in I_{1,\ldots,n}} b_\alpha \Phi_\alpha(\xi_1, \cdots, \xi_n) \end{aligned}, \quad (14)$$

where

$$I_{i_1,\ldots,i_s} = \begin{Bmatrix} \alpha \in (\alpha_1, \alpha_2, \cdots, \alpha_n) : \alpha_k = 0 \\ k \notin (i_1, \cdots, i_s), \forall k = 1, \cdots, n \end{Bmatrix}. \quad (15)$$

Calculated and sorted,

$$Y(\xi) = \sum_{\alpha \in I_{i_1,\cdots,i_s}} b_\alpha \Phi_\alpha(\xi_{i_1}, \ldots, \xi_{i_s}). \quad (16)$$

At the same time, the variance is obtained on both sides of (14) as follows:

$$Var\left[Y(\xi)\right] = D = \sum_{i=1}^{n} D_i + \sum_{1\le i<j\le n} D_{ij} + \cdots + D_{1,2,\ldots,n}. \quad (17)$$

Combined with the orthogonal relationship of (4),

$$D_{i_1,\ldots,i_s} = \sum_{\alpha\in I_{i_1,\cdots,i_s}} b_\alpha^2. \quad (18)$$

Thus, the Sobol first-order sensitivity index is as follows:

$$S_{i_1,\ldots,i_s} = \frac{D_{i_1,\ldots,i_s}}{D}, 1\le i_1<\ldots<i_s\le n; s=1,\ldots,n. \quad (19)$$

This equation represents the contribution of a single input to the output response variance.

The total sensitivity of Sobol is as follows:

$$S_i^T = S_i + \sum_{j<i} S_{j,k,i} + \cdots + S_{1,2,\cdots,n}, \quad (20)$$

which is the sum of the first-order sensitivity index of each input variable and the sensitivity indices of interaction between variables. Compared with the first-order sensitivity, this index also contains the influence of interaction among variables.

III. MULTICONDUCTOR TRANSMISSION LINES MODEL

The three-conductor transmission lines model with the infinite ground plane (IGP) as the reference conductor shown in Fig. 4 is used as the analysis object. It is the most general structure of MTLs and can be extended to any application scenario. The MTLs satisfies the assumption of uniformity, no conductor loss, and no surrounding dielectric loss. The cross-section of the transmission line is set as a small size, i.e., an electrically short transmission line. Only one transverse electromagnetic wave propagation mode is approximated on the transmission lines.

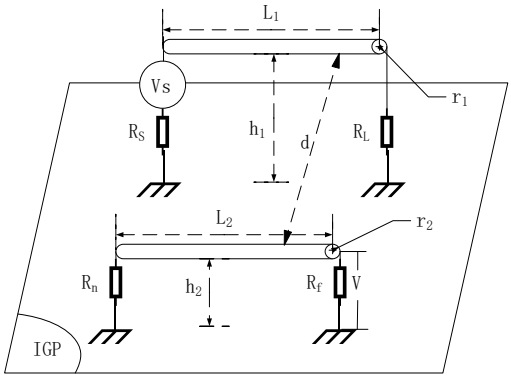

Fig. 4. Three-conductor transmission lines model.

The unit length inductance matrix and capacitance matrix of the three-conductor transmission lines can be obtained by the mirror analysis [30]. Then, the two-port transmission lines is described by the chain parameter matrix, and the current and voltage relationship at the port are characterized as follows:

$$\begin{bmatrix}\hat{V}(\ell)\\ \hat{I}(\ell)\end{bmatrix} = \psi\begin{bmatrix}\hat{V}(0)\\ \hat{I}(0)\end{bmatrix} = \begin{bmatrix}\hat{\phi}_{11} & \hat{\phi}_{12}\\ \hat{\phi}_{21} & \hat{\phi}_{22}\end{bmatrix}\begin{bmatrix}\hat{V}(0)\\ \hat{I}(0)\end{bmatrix}, \quad (21)$$

where $V(l)$, $I(l)$, $V(0)$, and $I(0)$ are the far-end crosstalk voltage, the far-end crosstalk current, the near-end crosstalk voltage, and the near-end crosstalk current, respectively, and ψ is the chain parameter matrix. For the transmission lines structure in Fig. 4, the generalized Thevenin theorem can be used to obtain the following:

$$\hat{V}(0) = \hat{V}_S - \hat{Z}_S\hat{I}(0), \quad (22)$$

$$\hat{V}(\ell) = \hat{Z}_L\hat{I}(\ell), \quad (23)$$

where $\hat{Z}_S$ and $\hat{Z}_L$ represent the near-end impedance matrix and far-end impedance matrix respectively and $\hat{V}_S$ represents the source voltage. Equations (22) and (23) are substituted in (21) to obtain the following:

$$I(0) = (\hat{\phi}_{12} - \hat{\phi}_{11} * Z_S - Z_L * \hat{\phi}_{22} + ZL * \hat{\phi}_{21} * Z_S)^{-1} * (Z_L * \hat{\phi}_{21} - \hat{\phi}_{11}) * V_S, \quad (24)$$

$$I(\ell) = \hat{\phi}_{21} * V_S + (\hat{\phi}_{22} - \hat{\phi}_{21} * Z_S) * I(0). \quad (25)$$

Equations (24) and (25) are substituted in (23) to obtain the far-end crosstalk voltage, and the correlation calculation of the chain parameter matrix is found in Ref. [31].

IV. NUMERICAL VERIFICATION AND DISCUSSION

The uncertainties of the crosstalk in the MTLs with random input parameters are analyzed using the transmission lines structure shown in Fig. 4. Assuming that the lengths of the two wires are equal $L=L_1=L_2$ and satisfy the uniform distribution [5.5 m, 6 m], the same radius $r=r_1=r_2$ obeys the normal distribution [0.7 mm, (0.1 mm)^2]. The equivalent height to ground $h=h_1=h_2$ obeys the uniform distribution [15 mm, 25 mm] and equivalent terminal impedance $R=R_L=R_f$ obeys the uniform distribution [45 Ω, 55 Ω]. The two wires are parallel and spacing d obeys the uniform distribution [5 mm, 10 mm]. The other parameters are set as constant: source voltage V_S=1 V, and source resistance $R_S=R_n$=50 Ω. The PCE model of the far-end crosstalk voltage in the frequency range of [1MHz, 100MHz] is established by using the equations in III and DA-SRSM.

Given the complex calculation of solving the crosstalk through the transmission lines equation, a high iteration degree upper limit p_{max}=20 is set. To ensure accuracy of the model, an error standard e_S=0.001 is set. Figure 5 shows the adaptive degree of each frequency band and the experimental error meets the requirements.

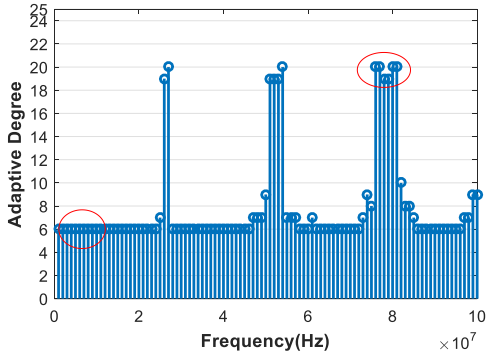

Fig. 5. Adaptive degree.

The adaptive degree varies at different frequencies. The adaptive degree is higher in [26 MHz, 27 MHz], [51 MHz, 54 MHz], and [76 MHz, 81 MHz], which indicates that the fitting model is more complex. The degree of other frequencies is relatively low, so the fitting model is simpler.

To verify the accuracy of the proposed model in the uncertainty analysis of crosstalk in MTLs, the first four statistical moments of the far-end crosstalk voltage V are calculated and compared with the results obtained by 10000-time MC methods as shown in Figs. 6 (a)–(d).

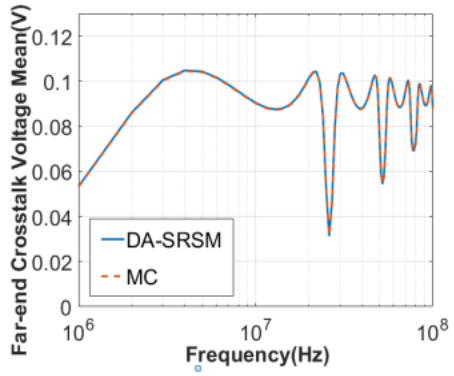

(a)

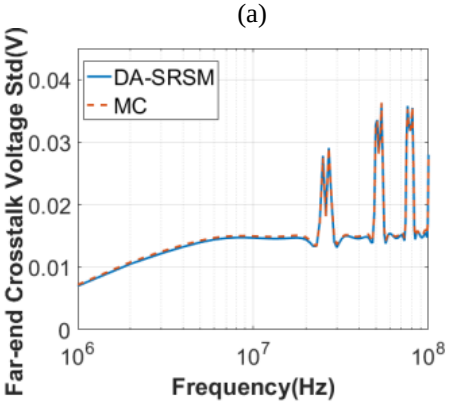

(b)

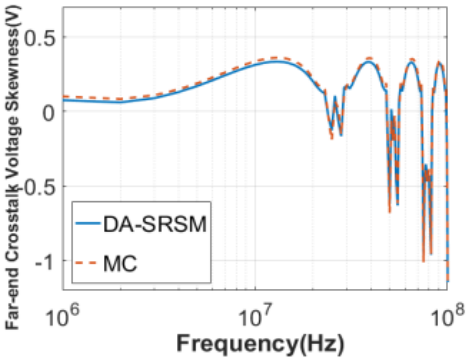

(c)

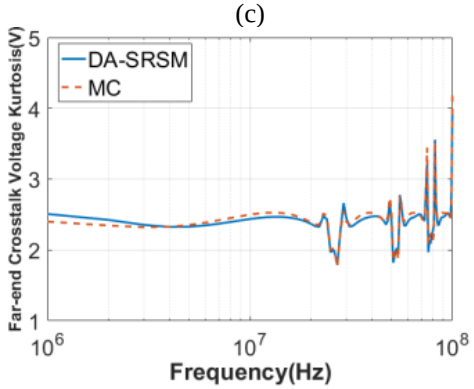

(d)

Fig. 6. Comparison of the results of the first four statistical moment of the far-end crosstalk voltage in the MTLs via DA-SRSM and the 10000-time MC method.

The first four statistical moments calculated by the proposed method have good consistency with the results calculated by 10000-time MC methods, which verifies the validity and accuracy of the proposed method. Figures 7 (a) and (b) further show the analysis of the error at the two frequency points of 40 MHz (p=6) and 80 MHz (p=20). The model error is the smallest at 6 degree and increases beyond 6 degree at 40 MHz. The model error decreases at 80 MHz, during which the p=20 model error is the smallest. The model meets the error standard at p=20. The accuracy and efficiency of the proposed method in full-band modeling are verified when the problem of crosstalk uncertainty of the complex MTLs is solved. The calculation times of the DA-SRSM and MC methods are shown in Table 1.

Table 1: Comparison of calculation times between DA-SRSM and MC methods

Calculation Method	Calculating Time (s)
DA-SRSM	537.3
MC	15012.4

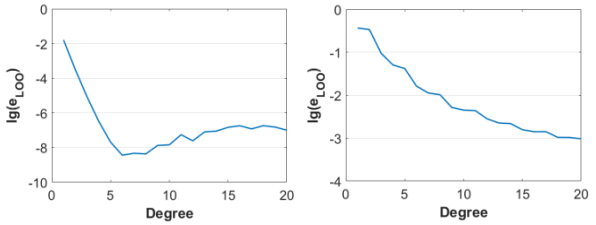

(a) (b)

Fig. 7. Model errors with iterative order at 40 MHz and 80 MHz via DA-SRSM.

Table 1 shows that to ensure accuracy of the model, the DA-SRSM greatly improves the computational efficiency compared with the MC method. The computer available for storage in this paper is 7.89 GB, the CPU clocked at 2.5 GHz, and no parallel operation is performed.

Next, the DA-SRSM is used to predict the failure probability of the EMC performance because of the crosstalk of the three-conductor transmission lines system shown in Fig. 4. The failure thresholds of the system in the [1 MHz, 10 MHz] and [75 MHz, 85 MHz] frequency intervals are all 0.12 V. Beyond the crosstalk voltage, the EMC performance of the system will be invalid. As shown in the red area in Fig. 5, the two sections represent the low-degree and high-degree models. The probability of the EMC performance failure of the MTLs system is calculated by DA-SRSM and compared with the 10000-time MC methods (Table 2).

Table 2: Comparison of EMC performance failure probability and calculated sample number in frequency ranges of [1 MHz, 10 MHz] and [75 MHz, 85 MHz]

Frequency	Method	Failure Probability	Number of Samples
[1MHz, 10 MHz]	DA-SRSM	0.0790	160
	MC	0.0806	10000
[75MHz, 85 MHz]	DA-SRSM	0.0540	210
	MC	0.0586	10000

Table 2 shows the failure probability obtained by DA-SRSM under the small sample calculation. The result is close to that obtained by the large sample calculation of the MC method. Compared with the MC method, DA-SRSM can considerably improve the calculation efficiency in two frequency intervals with certain calculation accuracy.

The two frequency points of 40 MHz and 80 MHz of the low-degree and high-degree models are selected based on Fig. 5. The probability density function of the far-end crosstalk voltage is calculated, and the results are compared with those of the 10000-time MC calculations, as shown in Figs. 8 (a) and (b).

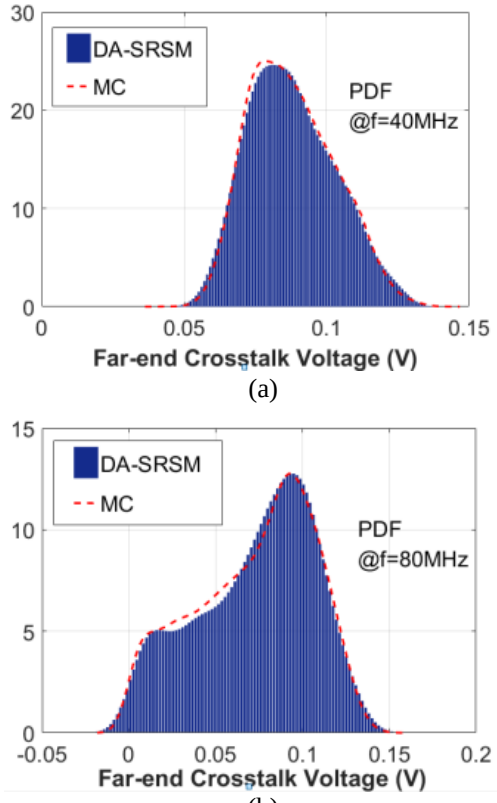

(a)

(b)

Fig. 8. Comparison of the far-end crosstalk voltage probability density function via DA-SRSM and MC method at 40 MHz and 80 MHz frequencies.

Figure 8 shows the probability density values obtained by DA-SRSM at both frequency points are consistent with those obtained by MC method. Thus, the accuracy of the proposed method is verified. The 40 MHz frequency has the highest probability density at 0.08 V, whereas the 80 MHz frequency has the highest probability density at 0.95 V. The probability density values of the same far-end crosstalk voltage response vary at different frequencies. The probability of failure at a certain frequency point can also be calculated by integrating the probability density curve.

The equations in Section II.D are combined to calculate the first-order and total sensitivities of each input variable at 40 MHz and 80 MHz. The result is compared with the results calculated by 10000-time MC, as shown in Figs. 9 (a)–(d).

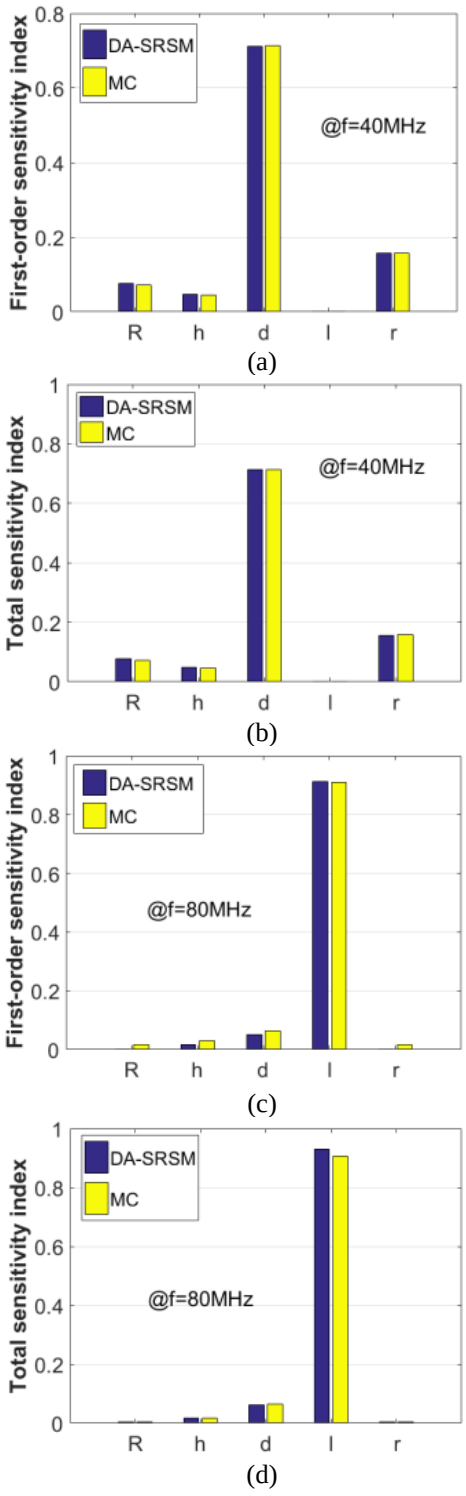

Fig. 9. Comparison of the first-order and total sensitivity indices of the input variables at 40 MHz and 80 MHz via DA-SRSM with the results calculated by the MC method.

Figure 9 shows the sensitivity results based on the DA-SRSM are consistent with those obtained by the MC method, which also verifies the accuracy of the proposed method. The first-order and total sensitivities at the same frequency point are the same, indicating that the interaction between input variables has little effect on the output response. At different frequencies, the results of the sensitivity indices vary greatly. The first-order and total sensitivities of lines spacing d are the highest at 40 MHz, which have the greatest effect on the change in the far-end crosstalk voltage. At 80 MHz, the first-order and total sensitivities of the conductor length L are the highest, whereas the sensitivity of d is very small. Thus, the influence of input variables on the far-end crosstalk voltage varies in the different frequency ranges. Comparisons of the above calculation time are shown in Table 3.

Table 3: Comparison of the program calculation time between DA-SRSM and MC method for calculating sensitivity

Frequency	Calculation Method	Calculating Time (s)
40MHz	DA-SRSM	4.3407
	MC	1604.3
80MHz	DA-SRSM	26.0113
	MC	1612.4

Table 3 shows that the calculation efficiency of Sobol sensitivity obtained by the DA-SRSM method is considerably higher than that of the MC method. To obtain the effects of the input variables in the [1 MHz, 100 MHz] frequency range on the variation of the far-end crosstalk voltage, the total sensitivity index at all frequency points is calculated (Fig. 10).

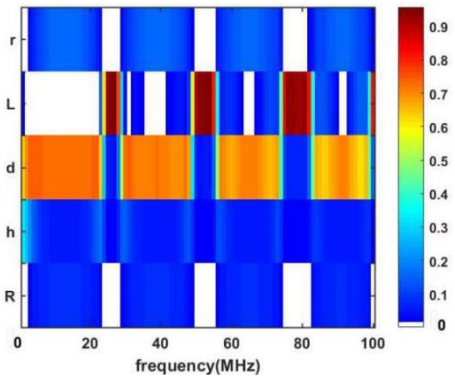

Fig. 10. Total sensitivity index of each input variable in [1 MHz, 100 MHz] interval via DA-SRSM.

Figure 10 shows the terminal impedance R, conductor height h, and wire radius r have a small effect on the output variation. The trend of the conductor spacing d and the wire length L is exactly the opposite. At [25

MHz, 27 MHz], [50 MHz, 54 MHz], [74 MHz, 83 MHz], L has considerable influence, d has a small degree of influence, and the other frequency bands is opposite. When designing the wiring of an electrical and electronic system or equipment where the above MTLs is located, if its main working frequency band is in the aforementioned three intervals, wire length L should be controlled strictly to ensure and the other parameters can be adjusted appropriately.

V. CONCLUSION

The DA-SRSM method is proposed for the statistical analysis of crosstalk in MTLs. The terminal impedance R, conductor-to-ground height h, conductor spacing d, conductor length L, and conductor radius R are set as random variables subject to certain distributions. The first four statistical moments and probability densities of the far-end crosstalk voltage are calculated and the model error is analyzed. The validity and accuracy of the proposed algorithm in the full frequency band are verified through a comparison with the MC method. DA-SRSM is also used to solve the problem of failure probability analysis of the EMC performance of an MTLs system. The failure probability of the EMC performance of the MTLs system is obtained quickly and accurately. The effects of random input variables at different frequencies on the variations of the far-end crosstalk voltage are also calculated by combining DA-SRSM with global sensitivity analysis of the Sobol method. This analysis is verified through the MC method. The proposed method is more accurate and efficient than the MC method in calculating the Sobol sensitivity indices. In conclusion, DA-SRSM can analyze the uncertainty of crosstalk in MTLs efficiently and accurately. Moreover, the proposed method can provide a theoretical basis and fast analysis for EMC problems, such as wire harness and cable crosstalk in electronic and electrical systems, which will have increasingly higher frequency and complexity in the future.

ACKNOWLEDGMENT

This work was supported in part by the National Natural Science Foundation of China under Grant 51707080, and in part by the Jilin Scientific and Technological Development Program under Grant 20180101032JC and Grant 20190103055JH.

REFERENCES

[1] V. Vulfin and R. Ianconescu, "Transmission of the maximum number of signals through a multi-conductor transmission line without crosstalk or return loss: Theory and simulation," *IET Microw. Antennas Propag.*, vol. 9, no. 13, pp. 1444-1452, 2015.

[2] R. Ianconescu and V. Vulfin, "Analysis of lossy multiconductor transmission lines and application of a crosstalk canceling algorithm," *IET Microw. Antennas Propag.*, vol. 11, no. 3, pp. 394-401, 2016.

[3] S. Shiran, B. Reiser, and H. Cory, "A probabilistic method for the evaluation of coupling between transmission lines," *IEEE Trans. Electromagn. Compat.*, vol. 35, no. 3, pp. 387-393, Aug. 1993.

[4] A. Ciccolella and F. G. Canavero, "Stochastic prediction of wire coupling interference," in *Proc. Int. Symp. Electromagn. Compat.*, Atlanta, GA, USA, pp. 51-56, Aug. 1995.

[5] B. Bellan, S. A. Pignari, and G. Spadacini, "Characterisation of crosstalk in terms of mean value and standard deviation," *IEE Proc.-Sci. Meas. Technol.*, vol. 150, no. 6, pp. 289-295, Nov. 2003.

[6] M. Larbi, P. Besnier, and B. Pecqueux, "Probability of extreme interference levels computed from reliability approaches: Application to transmission lines with uncertain parameters," *Int. Symp. Electromagn. Compa.*, Gothenburg, Sweden, pp. 648-655, 2014.

[7] M. Larbi, P. Besnier, and B. Pecqueux, "Probability of EMC failure and sensitivity analysis with regard to uncertain variables by reliability methods," *IEEE Trans. Electromagn. Compa.*, vol. 57, no. 2, pp. 274-282, 2015.

[8] L. Gao, Q. Yu, and D. C. Wu, "Probabilistic distribution modeling of crosstalk in multi-conductor transmission lines via maximum entropy method," *IEEE Access*, vol. 7, pp. 103650-103661, Aug. 2019.

[9] M. Wu, D. G. Beetner, T. H. Hubing, H. Ke, and S. Sun, "Statistical prediction of 'reasonable worst-case' crosstalk in cable bundles," *IEEE Trans. Electromagn. Compat.*, vol. 51, no. 3, pp. 842-851, Aug. 2009.

[10] M. S. Halligan and D. G. Beetner, "Maximum crosstalk estimation in lossless and homogeneous transmission lines," *IEEE Trans. Microw. Theory Techn.*, vol. 62, no. 9, pp. 1953-1961, Sep. 2014.

[11] A. C. Yücel, H. Bagci, and E. Michielssen, "An ME-PC enhanced HDMR method for effificient statistical analysis of multiconductor transmission lines networks," *IEEE Trans. Compon. Packag. Manuf. Technol.*, vol. 5, no. 5, pp. 685-696, May 2015.

[12] I. S. Stievano, P. Manfredi, and F. G. Canavero, "Parameters variability effects on multiconductor interconnects via Hermite polynomial chaos," *IEEE Trans. Compon., Packag., Manuf. Technol.*, vol. 1, no. 8, pp. 1234-1239, Aug. 2011.

[13] D. Xiu, *Numerical Methods for Stochastic Computations: A Spectral Method Approach*. Princeton, NJ, USA: Princeton Univ. Press, 2010.

[14] P. Manfredi, D. V. Ginste, I. S. Stievano, D. De Zutter, and F. G. Canavero, "Stochastic transmission lines analysis via polynomial chaos methods: An

overview," *IEEE Electromagn. Compat. Mag*., vol. 6, no. 3, pp. 77-84, 3rd Quart., 2017.

[15] I. S. Stievano, P. Manfredi, and F. G. Canavero, "Stochastic analysis of multiconductor cables and interconnects," *IEEE Trans. Electromagn. Compat*., vol. 53, no. 2, pp. 501-507, May 2011.

[16] S. Isukapalli, "Uncertainty analysis of transport-transformation models," *Ph.D. dissertation*, New Jersey, USA: Rutgers-The State University of New Jersey, 1999.

[17] G. Blatman, "Adaptive sparse polynomial chaos expansions for uncertainty propagation and sensitivity analysis," *Ph.D. dissertation*, Clermont Ferrand 2, 2009.

[18] G. Blatman and B. Sudret, "Adaptive sparse polynomial chaos expansion based on least angle regression," *J. Comput. Phys*., vol. 230, no. 6, pp. 2345-2367, 2011.

[19] S. Quicken, W. P. Donders, and E. M. J. V. Disseldorp, "Application of an adaptive polynomial chaos expansion on computationally expensive three-dimensional cardiovascular models for uncertainty quantification and sensitivity analysis," *J. Biomech. Eng*., vol. 138, no. 12, pp. 121010, 2016.

[20] F. Ni, P. Nguyen, and J. F. G. Cobben, "Basis-adaptive sparse polynomial chaos expansion for probabilistic power flow," *IEEE Trans. Power Syst*., vol. 32, no. 99, pp.1-1, Jan 2017.

[21] S. S. Isukapalli, A. Roy, and P. G. Georgopoulos, "Efficient sensitivity/uncertainty analysis using the combined stochastic response surface method and automated differentiation: Application to environmental and biological systems," *Risk Analysis*, vol. 20, no. 5, pp. 591-602, 2000.

[22] D. Xiu and G. E. Karniadakis, "Modeling uncertainty in flow simulations via generalized polynomial chaos," *J. Comput. Phys*., vol. 187, no. 1, pp. 137-167, 2003.

[23] W. Schoutens, *Stochastic Processes and Orthogonal Polynomials*. Springer Science & Business Media, vol. 146, 2012.

[24] M. Eldred, C. Webster, and P. Constantine, "Evaluation of non-intrusive approaches for wiener-askey generalized polynomial chaos," in *49th AIAA/ASME/ASCE/AHS/ASC Structures, Structural Dynamics, and Materials Conference*, pp. 1892, 2008.

[25] M. D. McKay, R. J. Beckman, and W. J. Conover, "A comparison of three methods for selecting values of input variables in the analysis of output from a computer code," *Technometrics*, vol. 42, no. 1, pp. 55-61, 2000.

[26] S. Hosder, R. Walters, and M. Balch, "Efficient sampling for non-intrusive polynomial chaos applications with multiple uncertain input variables," in *48th AIAA/ASME/ASCE/AHS/ASC Structures, Structural Dynamics, and Materials Conference*, pp.1939, 2007.

[27] B. Efron, T. Hastie, and I. Johnstone, "Least angle regression," *Ann. Stat*., vol. 32, no. 2, pp. 407-451, 2004.

[28] G. Blatman and B. Sudret, "An adaptive algorithm to build up sparse polynomial chaos expansions for stochastic finite element analysis," *Probab. Eng. Eng. Mech*., vol. 25, no. 2, pp. 183-197, 2010.

[29] M. Larbi, P. Besnier, and B. Pecqueux, "The adaptive controlled stratification method applied to the determination of extreme interference levels in EMC modeling with uncertain input variables," *IEEE Trans. Electromagn. Compat*., vol. 58, no. 2, pp. 543-552, Apr. 2016.

[30] C. R. Paul, *Introduction to Electromagnetic Compatibility*. John Wiley & Sons, 2006.

[31] C. R. Paul, *Analysis of Multiconductor Transmission Lines*. 2nd ed., New York, NY, USA: Wiley, 2008.